How sensitive is a dynamic ammonia synthesis process? Global sensitivity analysis of a dynamic Haber-Bosch process (for flexible seasonal energy storage)

Kevin Verleysen[a,b,c,*], Alessandro Parente[b,c], Francesco Contino[d]

[a] *Fluid and Thermal Dynamics (FLOW), Vrije Universiteit Brussel, Pleinlaan 2, 1050 Brussels, Belgium*
[b] *Combustion and Robust Optimization Group (BURN),Vrije Universiteit Brussel (VUB) and Université Libre de Bruxelles (ULB), 1050 Brussels, Belgium*
[c] *Université Libre de Bruxelles (ULB), Aero-Thermo-Mechanical Department (ATM), Avenue Franklin Roosevelt 50, 1050 Brussels, Belgium*
[d] *Institute of Mechanics, Materials and Civil Engineering (iMMC), Université catholique de Louvain (UCLouvain), Place du Levant, 2, 1348 Louvain-la-Neuve*

Abstract

The transition towards a sustainable energy sector depends on how we safely manage the transport and storage of energy to keep up with the demand. Large storage (TWh) of renewable energy can be accomplished by producing an energy carrier like ammonia. This power-to-ammonia production process overly depends on the stability of the ammonia reactor where any variations induced by uncertainties could have a large impact on the performance during its dynamic operations. To determine the effect of these variations, we need to identify which of the uncertainties have to be scrutinized during model design. The current work carries out the development of a dynamic Haber-Bosch process, implementing uncertainties in the model and performing an uncertainty quantification analysis on the process. Subsequently, the sensitivity indices quantify the impact of these uncertainties on the design during ramp-up. The global sensitivity analysis indicated that the reactor inlet temperature has the most considerable impact on the performance during ramp-up, where the hydrogen/nitrogen ratio has the second most significant impact. We see that the uncertainty on the

*Corresponding author
Email address: Kevin.verleysen@vub.be (Kevin Verleysen)

reactor inlet temperature dominates (87.8%) the overall standard deviation of the ammonia production. More precise control over the inlet temperature could reduce this impact on the standard deviation. The work can be extended by including a hydrogen and nitrogen production process while powering the full process with renewable power. We can then measure the effect of coupling renewables directly to the dynamic power-to-ammonia process and optimize the design under uncertainty.

Keywords: Stochastic dynamic systems, Uncertainty quantification, Haber-Bosch process, Seasonal hydrogen storage, Aspen Plus Dynamics

---

1. Introduction

The full integration of renewables in the power sector relies on two key aspects: assuring the grid's stability and the certainty that demand can be covered throughout the year. Wind and solar energy affect both aspects because of the intermittency of these respective energy sources in time over seconds, day-to-day and months. Therefore, developing and integrating affordable energy storage solutions to moderate this behavior is essential to transition to a sustainable power sector [1–4]. In general, which type of storage is needed depends on the capacity, storage time and application (power quality, grid support, load leveling or bulk storage). Batteries find their way to store solar power as an in-house application and improve the power quality in the grid, while pumped hydro storage offers support to power networks in the form of load-leveling [5, 6]. To cover the inequality between multiple months, we need to look at electrofuels that will enable us to convert Terawatt-hours (TWh's) of energy into a substance and store it for multiple months. This Power-to-Fuels (PtX) concept defines the possibility of performing this large-scale and long-term energy storage that is needed to avoid the curtailment of excess renewable energy. Hydrogen (H_2) created through water electrolysis is a key element in this PtX concept, allowing for the production and use of a CO_2-free fuel [3, 7–9]. However, the storage of pure renewable H_2 for several months is perceived as expensive where the energy car-

rier is difficult to transport over large distances [9–11]. Ammonia (NH_3) gained a growing interest due to its less energy-intensive liquefaction and cheaper storage cost than pure H_2 [9]. The Haber-Bosch Synthesis (HBS) process allows us to produce NH_3 commercially and maturely by combining renewable H_2 and nitrogen (N_2) obtained from the air under high pressures (between 100 bar to 250 bar) and high temperatures (from 350°C to 550°C) in the presence of a metal catalyst [12, 13].

The primary concern of utilizing this Power-to-Ammonia (PtA) process is assuring the durability of the reactor against fluctuations, e.g. thermal cycling [14–16], and adapt the design for its implicit off-design operations [17]. Modern NH_3 synthesis plants are conventionally designed for steady-state operations [18–20]. Traditional research evaluates the PtA design with deterministic linear models and demonstrates the independent effect of model parameters on the economic cost or performance with a sensitivity analysis. Morgan et al. performed this methodology on the net present value of an islanded wind-powered ammonia synthesis plant with design parameters, e.g. wind turbine size and ammonia plant size, and economic factors, e.g. project lifetime and interest rate [21]. The study of Nayak-Luke examined the sensitivity of the levelized cost of NH_3 by varying the ramp-up rate of the HBS loop, the ratio of wind and solar power powering the PtA process and the levelized cost of electricity [19]. Tripodi et al. examined the effect on the ammonia production by changing the model parameters and the catalyst configurations of an ammonia reactor and a Haber-Bosch synthesis loop [22]. As shown by these research papers, variations in the model and design parameters could significantly impact the economics and performance of the PtA process. Cheema et al. considered implicit variations (H_2/N_2 ratio, Argon concentration and mass flow rate) in the Haber-Bosch loop and ammonia reactor design to improve the flexibility on the operation and production of NH_3 in steady-state [13, 17]. This work considered that this flexibility provides a stable ammonia production at its off-design performance for large-scale energy storage. However, the dynamic operation of an ammonia synthesis loop can be significantly affected by changes in the H_2/N_2

ratio or by disturbances (in the feed and temperature) at the inlet of the HBS loop as is shown by Stephens et al. [23]. Gullberg et al. examined how these disturbances and changes in the inlet feed of the Haber-Bosch loop can be rejected and controlled during operation, at the expense of more complex control structures [24].

When exploiting the PtA system in practice, the simulated performance will ultimately diverge from the real one. This discrepancy is caused by disregarding the effect of uncertainties on the process [25, 26]. Neglecting the effect of uncertainties in chemical systems could lead to loss of optimal control [27–29], decrease in product quality [30], a poor economic system [31] or bad decision making in operation and planning [32]. Therefore, including uncertainties during design optimization, i.e. performing a Robust Design Optimization (RDO), enhances the model's reliability while minimizing the effect of uncertainties on the performance [33–37]. The work of Tejeda-Iglesias et al. [34] shows the benefits of RDO on an industrial sulfuric acid (H_2SO_4) plant for improving its daily profits under operating and economic uncertainties in steady-state. The advantages of RDO combined with a multi-scenario approach are also shown for a steady-state carbon capture process in the paper of Cerrillo-Briones et al. [33]. This RDO approach can be extended to dynamic models, e.g. optimizing the transient behavior of catalytic flow reactor [38], maximizing the production of chemicals under stochastic conditions [39] and designing a robust controller for various chemical processes [27–29, 31, 40]. To quantify the effect of uncertainties on the performance, we need to minimize the computational cost while attaining a high accuracy. The study of Bhonsale et al. [39] and Makrygiorgos et al. [41] show the advantages of using non-intrusive Polynomial Chaos Expansion-based (PCE) algorithms over brute-force Monte Carlo Simulations (MCS) for uncertainty quantification in dynamic models. This PCE algorithm can be enhanced by implementing advanced sampling methods to increase the precision of the UQ analysis [42]. The advanced techniques developed in Paulson et al. can be implemented to allow the PCE to capture singularities that can occur during a dynamic process [43]. However, no other study considers and quantifies the ef-

fect of these uncertainties on a Haber-Bosch plant during its dynamic operation. The study of Laššák et al. showed that parametric uncertainties cause different temperature profiles on the steady-state ammonia reactor model [44], leading to changes in the ammonia production or, worst-case, a shut down of the reactor. This knowledge gap can be filled by creating a dynamic Haber-Bosch loop and include operational and parametric uncertainties into the model. With a global sensitivity analysis, we can then quantify the effect of the uncertainties on the NH_3 production at each timestep during a dynamic simulation. The present paper describes the HBS loop design in Aspen Plus Dynamics, where operational and parametric uncertainties are integrated into the process. During a process ramp-up, the time-frozen PCE algorithm quantifies the effect of these uncertainties on the NH_3 production.

2. Methodology

This section introduces the creation of a flexible Haber-Bosch synthesis loop and the implementation of a catalyst model into the NH_3 reactor to store renewable energy. Afterward, operational and parametric uncertainties are described and justified according to literature. Finally, the global sensitivity analysis method, which quantifies the effect of the implemented uncertainties on the ammonia production, is presented.

2.1. Flexible Haber-Bosch synthesis loop

A regular Haber-Bosch plant with an autothermal reactor composes of four main elements: a compressor which pressurizes the synthesis loop, a reactor to convert the H_2 and N_2 gas into NH_3, a heat exchanger to heat the inlet stream of the reactor with the heat from the exothermic ammonia synthesis reaction and a separation system (via condensation or adsorption) to extract the ammonia from the process. The following exothermic reaction in the reactor occurs:

$$N_2 + 3H_2 \rightleftharpoons 2NH_3 \quad \Delta H_{reaction} = -46.0\,kJ/mol_{NH_3}, \tag{1}$$

where $\Delta H_{reaction}$ is the heat of reaction. A recycle and purge stream are in place to recuperate the unreacted H_2 and N_2 gas in the ammonia synthesis process and remove inert gases that would accumulate in the synthesis loop (Figure 1) [17, 45–47]. The challenge to operate the Haber-Bosch process for its renewable purpose (i.e. capture and storage of excess renewable energy) lies in preserving the integrity of the metal catalyst [6]. This component is sensitive to temperature fluctuations where the temperature directly affects the ammonia production throughout the reactor. Load variations will inherently occur for this storage system to the variable nature of renewables, where industrial Haber-Bosch plants are not designed for this purpose. These large-scale ammonia plants are also unable to operate below 50%-60% of their nominal load due to the temperature increase by the exothermic ammonia reaction exceeding safety limits [24, 48]. However, the patent of Ostuni [48] provides a way to safely decrease the reactor load by decreasing the purge flow rate, which accumulates inert gases and cools down the reaction; preventing the reactor from exceeding its temperature limit. Besides, a bypass over the heat exchanger provides direct control over the temperature to the inlet stream of the reactor without external heating and cooling systems (Figure 1) [49].

To simulate the Haber-Bosch process behavior, we developed an ammonia synthesis plant in Aspen Plus Dynamics, where the reactor model has been validated by Tripodi et al. using experimental results [22]. Our adopted Haber-Bosch model configuration is based on the design of a small-scale ammonia process described by Reese et al. (Figure 1) [26]. The design of [26] was adapted with a bypass to control the reactor's inlet temperature. In practice, the inlet reactor temperature is measured and rectified with the control valve, which controls the gas flow through the bypass. A heating system heats the incoming gas flow when performing a cold start-up of the plant [24, 26]. This entering gas flow provides a limitation to the valid range of the reactor model when going below the 50% load (to 10%-20%). Below this load, the reactor model deviates from the experimental results [22], where the plant performance prediction is not reliable as discussed in Tripodi et al. [50]. Therefore, the additional control

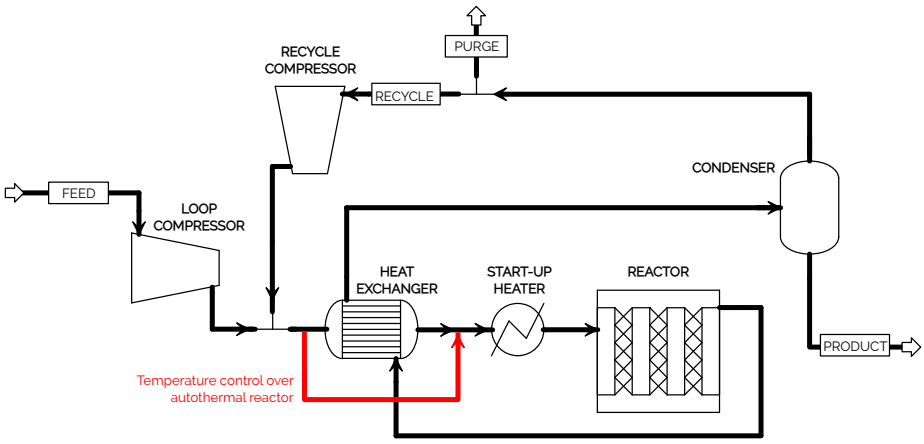

Figure 1: A loop compressor pressurizes the feed flow, where the flow is then mixed with the recycle flow. The combination of a heat exchanger and a bypass flow maintains control over the reactor's inlet temperature when load variations occur. Within this reactor, an exothermic reaction of hydrogen and nitrogen to ammonia takes place. The hot reactor outlet stream is cooled down and transferred to the condenser, where ammonia condenses. The unreacted gasses are partially purged and the remaining gas mixture is recycled.

elements to go below this 50% load were not integrated because these elements would need to control the reactor's temperature while keeping the flow rate at the inlet of the reactor within the valid range. For this particular reason, we considered a load below 50% out of the scope of this work.

The Haber-Bosch model is first created in Aspen Plus with the Redlich-Kwong-Soave-Boston-Mathias (RKS-BM) property method. Each component consists of material, energy and composition balances equations [51], where the convergence solver uses the Broyden method to solve the equations in steady-state. The parameters of all components were integrated into Aspen Plus and then exported to Aspen Dynamics with a flow-driven simulation where the Implicit Euler method was chosen as the dynamic solver. During the model simulations, we provide a feed of pure H_2 and N_2 at a temperature of 50°C and a pressure of 5 bar, where the loop compressor pressurizes the flow to 100 bar with an isentropic efficiency of 72% and mechanical efficiency of 100% (Figure 1). The flow is then adiabatically mixed with the recycle flow and heated

with the heat exchanger. Based on the nominal load size of the plant of 80 kg/h, an Aspen Plus optimization tool sized the heat exchange area to 6 m^2 to provide a flow of 400°C at the inlet of the reactor. The reactor sizing is based on the paper of [22], where we designed a single tube reactor with a length of 8 m, a diameter of 0.0404 m and 20 kg of wustite (with a density of 3250 kg/m^3). Below a nominal load of 80 kg/h, this temperature increases due to a higher residence time of the H_2/N_2 mixture in the reactor, which increases the exothermic reaction. This operation results in a higher temperature outlet flow going the heat exchanger [22]. The control valve of the bypass adapts the flow through the heat exchanger to keep the measured inlet temperature at 400°C. The product stream leaving the heat exchanger and entering the condenser is cooled down to a temperature of -20°C, which condenses the ammonia. The residual gas in the condenser (mainly H_2, N_2 and traces of NH_3) is purged for 4%, limiting the magnitude of the recycle flow. The recycled flow is then pressurized with a recycle compressor to 101 bar. In our dynamic model, we assume that the operating pressure of 100 bar is kept constant at all instants to avoid the limit cycle behavior. This assumption can be substantiated by inserting a control structure to the loop described by Gullberg et al. [24]. We added a PI controller to adapt the bypass flow over the heat exchanger while measuring the temperature that enters the start-up heater, which is sufficient for this operation [16]. We implemented a controller gain of 11.2% and an integral time of 10 min. The Aspen tuning process calculated these parameters by the internal model control tuning rule based on a step disturbance. This method allows to generate the proportional and integral control actions in the absence of implementing dead times in a robust way without overshoots and oscillations [51].

2.2. Catalytic reactor model

Different kinds of catalyst materials exist, where in traditional large-scale ammonia plants, iron-based catalysts are used for their economic benefits. To transition from a large centralized fossil-fueled HBS loop to a small-scale (isolated) electric Haber-Bosch, this traditional catalyst is incapable of functioning

under the renewable conditions (lower operational pressure, a dynamic supply of H_2 and higher safety risks) [52]. For this renewable purpose, a ruthenium catalyst shows better performance than iron catalysts to its higher activity, a H_2/N_2 ratio of 1.5 mol/mol (lower than the stoichiometric equilibrium of H_2/N_2 = 3 mol/mol) [22] and minor poisoning by oxygen [53]. A significant drawback of the ruthenium-based catalyst is the higher cost than the commercially available iron catalyst [11, 18]. As an alternative to iron and ruthenium, wustite is currently seen as the most durable and commercial material to withstand temperature variations at low operating pressures (around 100 bar) for this renewable purpose [54]. Because of this advantage, we created a dynamic reactor model in Aspen Plus Dynamics using the fugacity-based Langmuir-Hinshelwood-Hougen-Watson (LHHW) equation for the reaction rate (Equation 2) and adopted the kinetic parameters of a wustite catalyst, described by Tripodi et al. (Table 1) [22].

$$r = (k\ e^{-\frac{E}{RT}}) \frac{(K_{\text{Forward}} \prod_r f_r^{v_r} - K_{\text{Reverse}} \prod_p f_p^{v_p})}{(K_{\text{i}} \sum_i f_i^{v_i})^n} \tag{2}$$

This equation describes the relation between the reaction rate r in $\text{kmol/kg}_{\text{cat}}\text{s}$, the kinetic factor k in $\text{kmol/kg}_{\text{cat}}\text{s}$, the activation energy E in J/mol, temperature T in K, the gas constant R (8.314) in J/molK, the fugacity of a component f^{v_x} ($v_x \in \{N_2, H_2, NH_3\}$), the forward K_{Forward}, reverse K_{Reverse} and adsorption K_{i} equilibrium constant. The adsorption equilibrium constant is non-existent for the wustite material, where this term is negated with the exponent $n = 0$. The forward and reverse equilibrium constants are calculated in Aspen with the following equation:

$$\log(K_z) = A_z + B_z/T + C_z \ln(T) + D_z T, \tag{3}$$

where A_z, B_z, C_z and D_z are constants described for the driving force K_z ($z \in \{\text{Forward}, \text{Reverse}\}$) in Table 1. We recreated the ammonia synthesis loop from Tripodi et al. and validated the kinetic reactor models with different cases described in Table 3 of the paper and Table S1 of the supplementary document. Here, the most significant relative error of 1.58% was found on the ammonia

mole fraction in case 4 of Table 3. The sensitivity of the recycle stream invokes this error on the ammonia mole fraction, as described in the supplementary data of Tripodi et al. [22]. The design parameters and the region of operation of the renewable Haber-Bosch are based within the valid region of the kinetic model of the wustite catalyst.

Table 1: Kinetic parameters for wustite catalyst integrated in Aspen Plus Dynamics [22].

	H_2	N_2	NH_3		Remark
Stoichiometry	-3	-1	2		LHHW equation
	k [kmol/kg$_{cat}$s]	n	E [J/mol]		Remark
Kinetic cst.	$7.47 \cdot 10^8$	0	$1.88406 \cdot 10^8$		Fugacity based
Driving force	A	B	C	D	$v_x = [H_2; N_2; NH_3]$
Forward	-7.8	9218	-5.42	$7.8 \cdot 10^{-4}$	[2.25; 1; -1.5]
Reverse	2.88	0	0	0	[-0.75; 0.0; 0.5]

2.3. Implemented uncertainties on the design

The goal of this research is to assess the sensitivity of the NH_3 production under uncertainty during ramp-up. There are two types of uncertainties that could impact the performance in practice, namely operational and parametric uncertainties. Operational uncertainties originate from variations that occur during operation, going beyond the predefined designed process, e.g. different H_2/N_2 ratio than the theoretical equilibrium or temperature variations in the system to measurement errors [40, 45]. Parametric uncertainties are caused by errors on the model parameter, e.g. reaction enthalpy and catalyst density. This type of uncertainty affects the prediction of the nonlinear behavior of the model [30, 38, 40, 44].

We integrated three operational uncertainties into the design: a variant temperature at the reactor inlet, a variant temperature in the condenser's cooling and an uncertain H_2/N_2 ratio at the HBS inlet feed. Reactor temperature fluctuations are observed in the experimental results of a small-scale ammonia synthesis plant described by Reese et al. [26]. The origin of these variations was associated with the difficult control of the plant [26], which have a considerable impact on the ammonia plant's behavior and performance of the ammonia plant [55]. Because of the sensitivity of a real ammonia plant by the inlet temperature, we integrated this fluctuation as an uncertainty at the set point of the PI controller, which controls the flow rate through the bypass. We defined the source of uncertainty here as the combination of temperature measurement uncertainty [56] and the inadequate control over the plant [26]. We chose a gaussian distribution for the temperature fluctuation at the reactor inlet (T_{reactor}) with a mean of 400°C and a standard deviation of 1.67% of the mean (6.67°C), which correspond to the relative temperature surges of the plant of Reese et al. [26]. We assumed the same temperature variation could occur at the condenser, where the incoming flow is cooled to a set temperature, but a measurement error and difficult control over this temperature can affect the actual temperature. For the temperature fluctuation in the condenser ($T_{\text{condenser}}$), the mean and standard deviation of this gaussian uncertainty is respectively -20°C and 1.67% of the mean (0.33°C). The uncertainty ranges in the reactor inlet temperature and the condenser temperature are also corresponding to real temperature uncertainty measurements, where examples can be found in the report of Scheller et al. [56]. Besides the temperature fluctuations, a H_2/N_2 ratio variation occurred during the plant's operation in Minnesota due to independent fluctuations in the H_2 and N_2 supply [26]. It was observed that the buffer tank between the air separation unit (providing the nitrogen supply) and the HBS process did not sufficiently damp out the fluctuations. In addition, the electrolyzer feeding the HBS process with H_2 did not feed the system with the required rate (underproduction of H_2). A uniform probability density function is adopted for the H_2/N_2 ratio with a minimum and maximum range of 2.5 mol/mol to 3.0

mol/mol.

We want to quantify the effect of small changes on two model parameters for the parametric uncertainties, namely the reaction enthalpy and the wustite catalyst density. The work of Laššák et al. tested the effect of a variation of the heat of reaction ($\Delta H_{reaction}$) on the output temperature of an ammonia reactor in steady-state conditions [44]. This variation is also adopted as a parametric gaussian uncertainty in the reactor, where the mean of the reaction enthalpy is $-46\,kJ/mol_{NH_3}$ and the standard deviation is 5% of the mean ($2.3\,kJ/mol_{NH_3}$). In Gramatica's work, we observe that the density of the catalyst can have small changes according to its real theoretical one, where a maximum variation of 3% in mass density can occur due to different catalyst particle sizing [57]. For this reason, we integrated this uncertainty on the wustite catalyst density ($\rho_{wustite}$) with a gaussian distribution where the mean is $3.25\,g/cm^3$ and the standard deviation is 1% of the mean ($3.25 \cdot 10^{-3}\,g/cm^3$). The implemented uncertainties in the Haber-Bosch synthesis loop are summarized in Table 2 and visualized in Figure 2.

Table 2: Summary of the implemented operational and parametric uncertainties into the dynamic Haber-Bosch synthesis loop in Aspen Plus Dynamics. The uniform distribution with a mean and standard deviation corresponds to the uniform distribution with a range of 2.5 mol/mol and 3 mol/mol [58].

Operational uncertainty	Distribution	Mean	Standard deviation	Unit
H_2/N_2	uniform	2.75	0.14	mol/mol
$T_{reactor}$	gaussian	400	6.67	°C
$T_{condensor}$	gaussian	20.0	0.33	°C

Parametric uncertainty	Distribution	Mean	Standard deviation	Unit
$\Delta H_{reaction}$	gaussian	-46.0	2.30	kJ/mol_{NH_3}
$\rho_{wustite}$	gaussian	3.25	$3.25 \cdot 10^{-3}$	g/cm^3

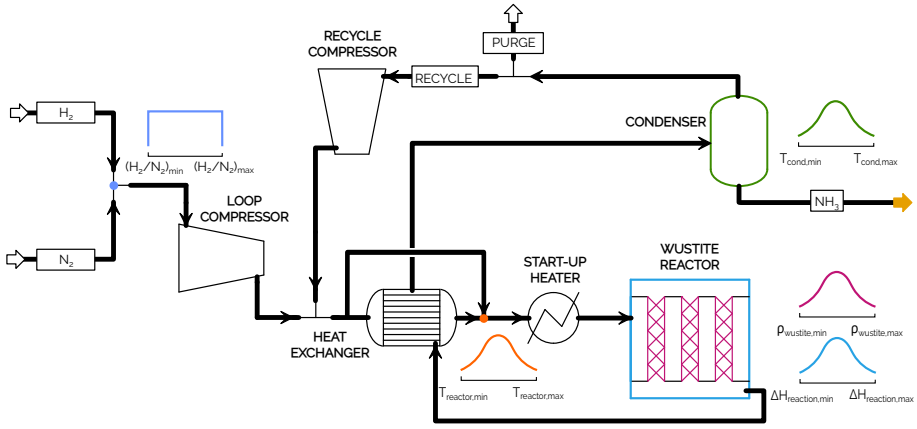

Figure 2: Five uncertain parameters are implemented in the dynamic Haber-Bosch model, where the H_2/N_2 ratio has a uniform distribution and the other uncertainties have a gaussian distribution. The H_2/N_2 ratio, the temperature at reactor inlet and in the condenser are considered operational uncertainties and the heat of reaction and wustite density are parametric uncertainties.

2.4. Global sensitivity analysis

A sensitivity analysis that quantifies the combined effect of all the uncertain parameters on the performance of simulated systems was performed [41, 59, 60]. The contribution of each uncertainty to the variation of the NH_3 production can analytically be quantified through the so-called Sobol' decomposition. From this decomposition, the Sobol' indices S_u can be extracted which are defined as the ratio of the partial variance D_u and the total variance D:

$$S_u = \frac{D_u}{D}, \tag{4}$$

where u is the index set of the implemented uncertainties [60]. The total Sobol' index S_i^T quantifies the total impact of each uncertainty i on the total variance D by considering every possible interaction between all of the stochastic input parameters that contain uncertainty i [41, 59, 60]:

$$S_i^T = \sum_{i \in u} S_u. \tag{5}$$

The partial and total variance are traditionally derived by evaluating the computational model M with an MCS. For a non-intrusive UQ analysis of static

deterministic models, MCS takes 10^4 to 10^6 evaluations to get accurate statistics on the moments (mean and standard deviation) [35, 37, 39, 41, 44, 59, 61, 62]. The uncertainty propagation of our dynamic Haber-Bosch model would result in a computational time of approximately 200 days to converge with 10^4 runs. Alternatively, the Polynomial Chaos Expansion (PCE) provides an efficient alternative over MCS because the Sobol' indices can analytically be derived while avoiding the computational cost of running excess time-expensive models [59, 60, 63] and iteratively determine the Sobol' indices [64]. PCE creates a metamodel $\hat{M}$ by constructing a truncated series of orthogonal polynomials Ψ_i and their corresponding coefficients a_i with an order P to approximate the real response of model M to an input $\boldsymbol{\xi}$ [37, 65, 66]:

$$\hat{M}(\boldsymbol{\xi}) = \sum_{i=0}^{P} a_i \Psi_i(\boldsymbol{\xi}) \approx M(\boldsymbol{\xi}). \tag{6}$$

These orthogonal polynomials Ψ_i are Hermite polynomials for gaussian distribution and Legendre polynomials for uniform distributions following the Askey scheme [29, 59, 67]. We refer to Example 3.3.3 of Wu et al. on combining different orthogonal polynomials when constructing the metamodel [59]. This static UQ analysis can then be extended to the so-called time-frozen PCE, where the PCE algorithm creates a metamodel at each timestep [41, 68]. To analytically determine the mean and standard deviation of the NH_3 production at a time t in a computationally efficient way, we refer to the work of [41, 43, 68–71]. Afterward, the Leave-One-Out (LOO) cross-validation procedure computes the error between the metamodel $\hat{M}$ and the computational model M [41, 43].

So obtaining the global sensitivity of complex dynamic systems used in the field of energy capture and storage provides us with a measure of how the operational and parametric uncertainties impact the performance of such a plant during operations [61]. To efficiently determine the Sobol' indices, the use of PCE is advantageous over MCS for running computational expensive dynamic models.

3. Results and discussion

In this section, we discuss the results of the dynamic Haber-Bosch model in Aspen Plus Dynamics. We first evaluate the deterministic performance of the dynamic model during ramp-up. Then we compare the stochastic model with the deterministic one by describing the change in the evolution of the mean and standard deviation during ramp-up. Next, the total-order Sobol' indices and the probability density functions over time are presented and discussed. Afterward, we provide a scenario with increased ramp-up rates and discuss the results. Finally, we provide our suggestions to minimize the impact of the uncertainties on the dynamic Haber-Bosch process.

3.1. Performance of deterministic model during ramp-up

According to Armijo et al. [10], the ramp-up of the Haber-Bosch process is limited by 20% of the nominal load per hour. Therefore, we ramped up the process from a partial load of 50% to 100% (from 40 kg/h to 80 kg/h) over 150 minutes. This ramp-up resulted in an increasing output flow rate of the Haber-Bosch loop from 30.8 kg/h to 50.4 kg/h, where 99.9% of this mass output flow rate consists of NH_3 (Figure 3). Although a linear increase in supply is accomplished, the synthesis loop's non-linear behavior results in the saturation of the ammonia production around 50.4 kg/h. The saturation originates from the increasing mass flow inside the loop process, which reduces the contact time between the H_2/N_2 mixture and the wustite catalyst. This contact time reduction affects the process in a twofold aspect: first, it decreases the NH_3 synthesis directly, and second, the accumulation of unreacted gas increases the mass flow inside the loop process, reducing the contact time furthermore [13, 22, 24]. The ramification of the two effects is observed inside the wustite reactor, where the output temperature decreases when the ammonia reactor's load increases (Figure 4). The decreasing output temperature is caused by the reduction of NH_3 conversion resulting in a lower heat release from the exothermic reaction. To optimize the ammonia synthesis point of operation, we can shift towards a lower H_2/N_2 ratio at higher flow rates [24].

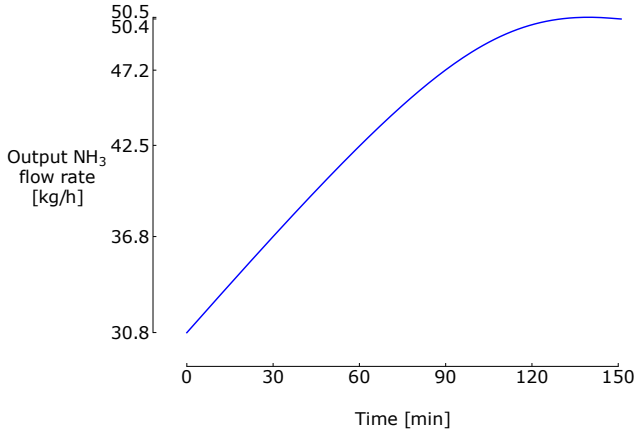

Figure 3: To the Haber-Bosch's non-linearity, the system's output increases in a non-linear way when ramping up from a load of 40 kg/h to 80 kg/h with a H_2/N_2 ratio of 3. The output saturates around a maximum mass flow rate of 50.4 kg/h, where a slight overshoot occurs when reaching the maximum capacity of the NH_3 process.

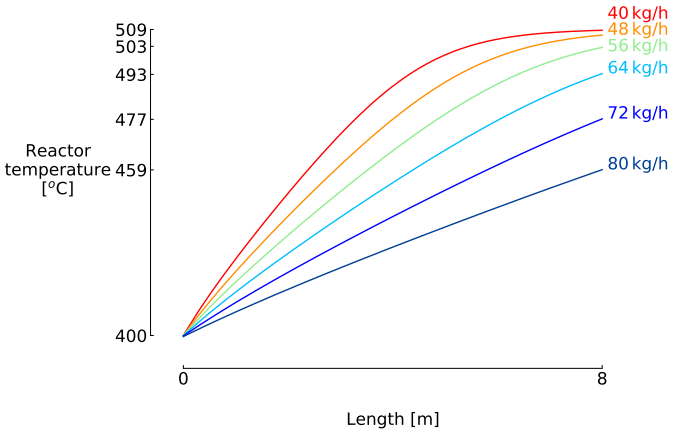

Figure 4: The increasing feed flow rate (with H_2/N_2 ratio of 3) decreases the contact time between the gas mixture and the catalyst, reducing the heat release of the exothermic reaction. This effect reduces the ammonia synthesis efficiency and causes a decrease in output temperature by 50°C, resulting in the ammonia output's saturation to 50.4 kg/h.

As observed in the Aspen Plus Dynamics model, reducing the H_2/N_2 ratio reduces the decreasing temperature output of the reactor, which is bene-

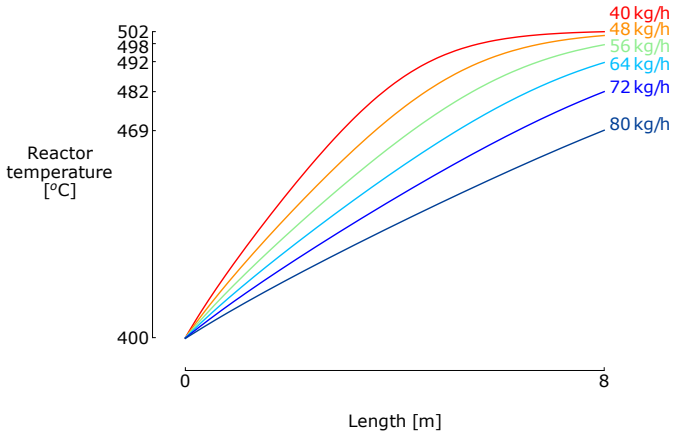

Figure 5: The increasing feed flow rate at a H_2/N_2 ratio of 2.5 decreases the contact time between the gas mixture and the catalyst, but the effect on the output temperature is limited by 33°C. The smaller decrease in output temperature by the lower H_2/N_2 ratio results however in a reduced NH_3 production.

ficial when operating in stochastic conditions preventing a reactor shutdown (Figure 5). However, a lower H_2/N_2 ratio impacts the performance of the Haber-Bosch loop on another aspect, namely the NH_3 synthesis decreases to less favorable equilibrium conditions, which decreases the total NH_3 production (Figure 6). The relative difference between the different NH_3 production conditions changes depending on the Haber-Bosch loading. At a load of 40 kg/h, the relative NH_3 production is 11.0%, where at a load of 80 kg/h, this difference is 4.2%. The reason for this smaller relative difference lies in the influence of the contact time between the gas mixture and catalyst in combination with a favorable equilibrium condition of the different H_2/N_2 ratios, as is previously explained.

3.2. Performance of stochastic model during ramp-up

In this part, we implemented the operational and parametric uncertainties on the dynamic Haber-Bosch process and performed a global sensitivity analysis on the model during ramp-up to quantify the collective effect of uncertainties on the NH_3 production. We carried this global sensitivity analysis out with

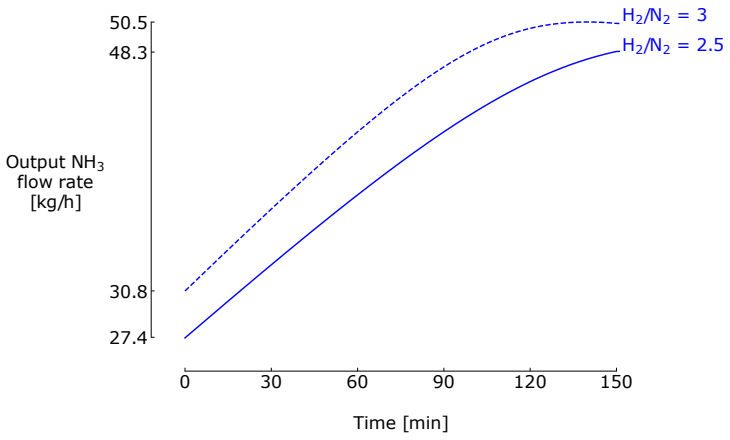

Figure 6: In comparison, less NH_3 is produced by the Haber-Bosch synthesis loop at a lower H_2/N_2 ratio than when the process operates at the theoretical equilibrium of 3 mol/mol. However, the relative difference between the NH_3 productions is more considerable at a low flow rate because of higher contact time favoring the reaction of a H_2/N_2 close to 3 mol/mol than at higher flow rates (with a relative difference of 4.2%).

our in-house developed PCE Python script [67], which invoked the Aspen Plus Dynamics model via a Matlab-Simulink connection [72]. In this work, we used a polynomial order p of 3 to create the PCE metamodel from 112 samples and extract the necessary information at a timestep of 0.1 min. The highest LOO that we observe is 0.015, which is found sufficient to extract the mean and standard deviation accurately.

The sensitivity analysis of each timestep reveals that the mean ammonia production increases from 29.1 kg/h to 49.1 kg/h during this transition. At the start of the ramp-up, the mean ammonia production lies symmetrically between the deterministic values of the NH_3 productions for different H_2/N_2 ratios (Figure 7). This symmetry indicates that the operational uncertainty on the H_2/N_2 ratio has a considerable influence over the process's output at lower loads. On the other hand, this symmetry disappears for the plant at its maximum load, where at the same time, the standard deviation increases from 1.0 kg/h to 5.3 kg/h (Figure 8). This observation implies that the dynamic Haber-Bosch system is more sensitive to the implemented uncertainties at a

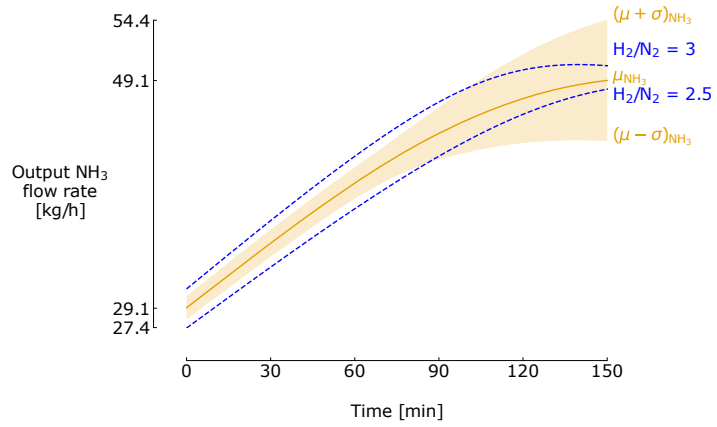

Figure 7: During the load ramp-up from 40 kg/h to 80 kg/h, the mean ammonia production elevates from 29.1 kg/h to 49.1 kg/h. The standard deviation around the mean increases due to the amplifying effect of the uncertainty on the reactor inlet temperature fluctuation. For the nominal load of 80 kg/h load, the temperature variation has the largest negative effect over the ammonia synthesis efficiency at this operational point.

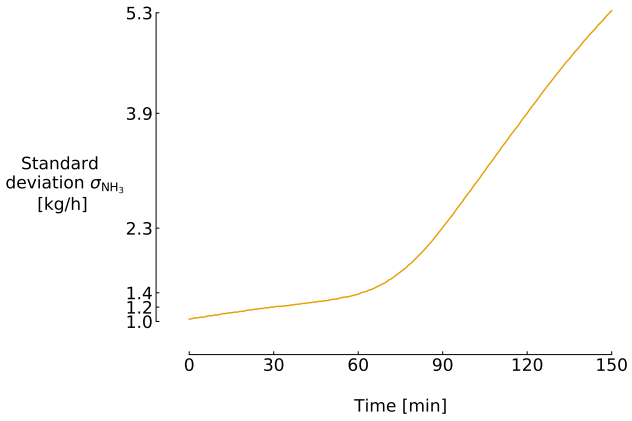

Figure 8: The increase in load from 40 kg/h to 80 kg/h results in a higher standard deviation of the ammonia production. This increase shows that the Haber-Bosch system is more sensitive towards the implemented uncertainties at higher loads.

load of 100% than at 50%. This effect originates from the gas mixture's short residence time, where the temperature variation at this point of operation affects the efficiency of the ammonia synthesis inside the reactor the most. Because

of this significant increase in standard deviation, the NH_3 production could be considerable impacted at higher loads, leading to a larger recycle flow rate and a higher recycle compressor duty.

This behavior can be explained by looking at the sensitivity indexes of each timestep (Figure 9). At the beginning of the ramp-up, the H_2/N_2 ratio (0 min) dominated the standard deviation with 92.0%, increases shortly (30 min) to 95.2% where it then decreases to 4.4% (150 min). During this evolution, the reactor's inlet temperature variation becomes the dominant source of uncertainty due to the short residence time of the H_2 and N_2 gas mixture in the reactor. This results in a less efficient NH_3 reaction to occur at non-ideal equilibrium condition (H_2/N_2 ratio below 3 mol/mol). The residual uncertainties (condenser temperature, catalyst density and heat of reaction) remain below 5.6%. The uncertainty quantification at different timesteps shows that these three uncertainties can be excluded for future global sensitivity analyses. The probability density function of the output changes according to the load sizing and the dominance of the uncertainties (Figure 10). Throughout the plant's

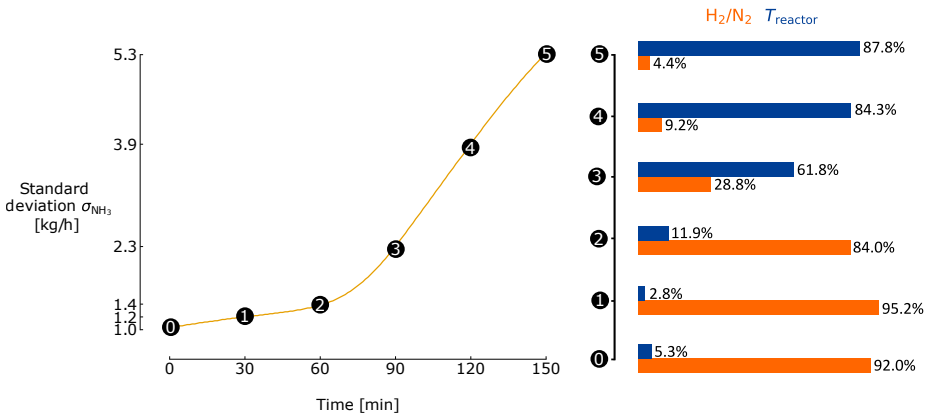

Figure 9: The increase in load from 40 kg/h to 80 kg/h results in a higher standard deviation of the ammonia production due to the more dominant effect of the temperature fluctuation at the reactor inlet. The Sobol' indices evolve during the ramp-up, where the H_2/N_2 ratio dominates the standard deviation with 92.0% and decreases to 4.4%. The temperature fluctuation becomes then the dominant source of variation with 87.8%.

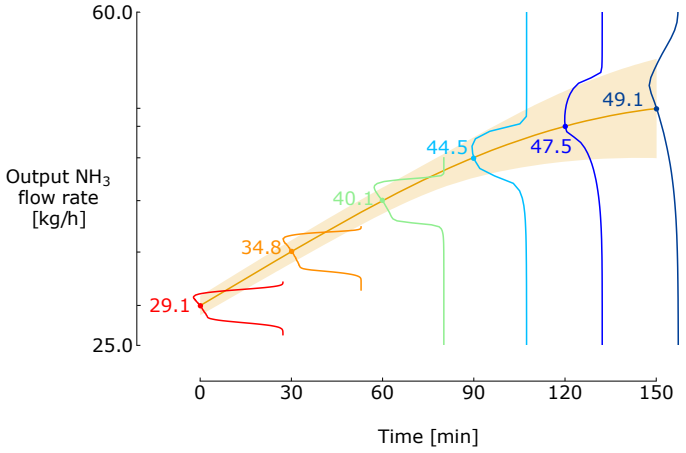

Figure 10: The probability density functions change shapes throughout the plant's ramp-up over time. At lower loads, the NH_3 production lies closer around the mean and is more certain, while at higher loads, the probability density functions around the mean stretch.

ramp-up, we examine the change in the probability density functions at each timestep of 30 min. At lower loads, we observe a high probability of producing NH_3 around the mean, where at higher loads, the probability of producing ammonia around the mean decreases and spreads. We identify that the inlet reactor temperature has a positive and negative effect on the ammonia production. A higher NH_3 production is achieved when the temperature at the inlet of the reactor is increased, when a lower temperature at the inlet reactor is supplied, the NH_3 production decreases due to less favoring ammonia kinetics under stochastic conditions.

To rule out the dominant effect of the inlet temperature uncertainty, we can consider operating within the range where the standard deviation has not a significant impact on the ammonia production. For this reason, we investigate with a global sensitivity analysis the effect of an increased ramp-up rate below this load of 64 kg/s. For this case, we assume a hypothetical ramp-up rate of 60% and 120% of the nominal load per hour. We set a load change of 50% to 65% and 50% to 80% in 15 min each time in this scenario. For the PCE metamodel, we used a polynomial order p of 3 with 112 samples. The maximum LOO that

was observed is 0.013, which is considered sufficient to extract the statistics accurately.

For this case, we notice that the mean and standard deviation do not change for the higher ramp-up and -down rates while observing no transient responses (Figure 11). This effect is linked to the size of the Haber-Bosch, which is

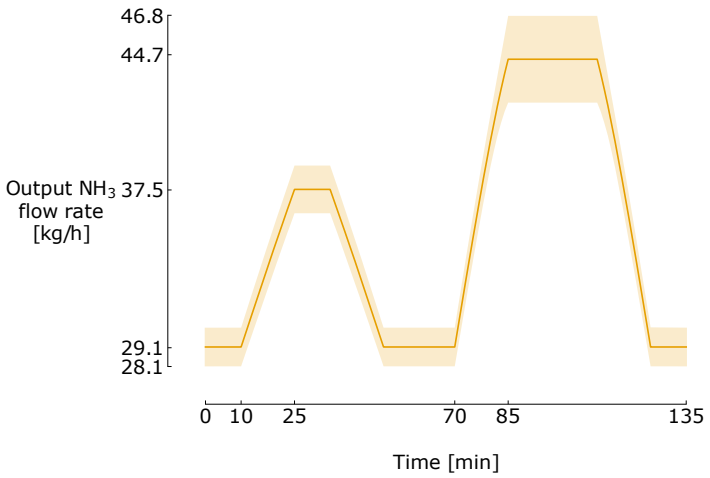

Figure 11: The consecutive ramp-ups from 40 kg/h to 52 kg/h and from 40 kg/h to 64 kg/h do not show any transient responses to the small reactor volume. The mean and standard deviation do not deviate from the values observed during the single ramp-up scenario.

considerably smaller than industrial reactors described in literature [16, 73–76]. The paper of Morud et al. shows the ammonia production dynamics is related to the volume, the number of reactors and the total residence time of the reactant gas for an industrial HBS process [16]. We distinguish that the implemented ramp-up and -down rates are slower than the dynamics of the reactor and the chosen PI controller. Here, we perceive that the HBS process can be used for higher ramp-ups until 80% while avoiding large standard deviations during operation. In practice, the sudden increase of the temperature profile could affect the reactor operation or damage the catalyst [77].

By evaluating the stochastic dynamic system with the time-frozen PCE, we recognize that the current designed Haber-Bosch system is not suitable for a

load approximately above 64 kg/s (80%) at this non-ideal condition. Overall, this process could reach lacking efficiencies at moments when renewables are abundantly available. The HBS process can only operate quickly and securely between 50% and 80% of the nominal load. In this range, the H_2/N_2 ratio and the reactor inlet temperature have the largest impact but only affects the ammonia production with a maximum standard deviation of 2.3 kg/h. Above this limit, the inlet temperature greatly influences the standard deviation of the ammonia process. To limit the effect of the temperature variation, a more accurate measurement sensor can reduce the effect on the ammonia production [45]. Alternatively, a suitable state estimation process, e.g. (extended) Kalman filters [78] or moving horizon estimation [79], catches the effect of these measurements uncertainties on controllers during load changes. The paper of Valipour et al. demonstrated that these techniques combined with a nonlinear model predictive control provides an effective way to control stochastic processes without imposing a computational expensive task during real-time operation [79]. For the uncertainty of the H_2/N_2 ratio, a shift of the probability density function around 3 mol/mol can significantly improve the system's performance. However, this shift would result in a large electrolyzer stack producing more hydrogen than necessary to reach the optimal equilibrium condition. Another solution is to integrate a second reactor after the wustite reactor. This secondary catalyst can boost the ammonia production at non-ideal chemical equilibrium conditions [22]. A ruthenium catalyst is seen as the most efficient way to solve this problem but would increase the cost of the PtA plant [54].

4. Conclusion

Stochastic parameters inherently influence the Power-to-Ammonia process for the capture and seasonal storage of renewable energy. As observed in the paper of Reese et al. [26], uncertainties affect the ammonia synthesis process during operations. The sources of uncertainties constitute measurement errors, difficult control or stochastic model parameters. Creating a dynamic model

and introducing the stochastic variables upon the model imitates the unwanted behavior and the effect on the system's performance. With the time-frozen Polynomial Chaos Expansion technique, the effect of these operational uncertainties (variations on the H_2/H_2 ratio, inlet reactor temperature measurement and condenser temperature measurement) and parametric uncertainties (heat of reaction and wustite density) was quantified during the plants' ramp-up from 50% to 100% of the plants' nominal load. We observed that the mean NH_3 mass flow rate increases, but the Haber-Bosch plant's sensitivity increases considerably when reaching the nominal load under the non-ideal conditions. The sensitivity indexes quantify the effect of the uncertainties on the ammonia production. We observed that a higher ramp-up rate does not affect these results within this designed HBS process. The H_2/N_2 ratio dominates the ammonia production at the start of the ramp-up, where the inlet temperature begins to dominate the process during the plants' ramp-up. This temperature variation dominates this result and can be reduced by limiting the temperature error with a more precise sensor or with a state estimation scheme combined with a suitable process controller. On the other hand, solving the effect of the H_2/N_2 ratio uncertainty would require a higher investment cost, where a higher supply of H_2 is needed to increase the range of this uncertainty. An alternative solution is the use of a second reactor with a ruthenium catalyst. Future work entails the Haber-Bosch plant's global sensitivity ramping up from lower loads (below 50%) and performing combinations of increasing and decreasing the plants' load according to a renewable power supply profile. Also, a more robust design (i.e. less sensitive to uncertainties) is sought to allow an efficient Haber-Bosch process under variable load, so the application of this process for seasonal hydrogen storage can advance.

5. Acknowledgment

Aspen Plus Dynamics was used under academic license.

References

[1] IEA, Perspectives for the Clean Energy Transition (2019).
URL https://www.iea.org/publications/reports/PerspectivesfortheCleanEnergyTransition/

[2] J. Fuhrmann, M. Hülsebrock, U. Krewer, Energy Storage Based on Electrochemical Conversion of Ammonia, in: Transition to Renewable Energy Systems, Wiley-VCH Verlag GmbH & Co. KGaA, Weinheim, Germany, 2013, pp. 691–706. doi:10.1002/9783527673872.ch33.
URL http://doi.wiley.com/10.1002/9783527673872.ch33

[3] V. Dias, M. Pochet, F. Contino, H. Jeanmart, Energy and Economic Costs of Chemical Storage, Frontiers in Mechanical Engineering 6 (2020) 21. doi:10.3389/fmech.2020.00021.
URL https://www.frontiersin.org/article/10.3389/fmech.2020.00021/full

[4] G. Limpens, H. Jeanmart, Electricity storage needs for the energy transition: An EROI based analysis illustrated by the case of Belgium, Energy 152 (2018) 960–973. doi:10.1016/j.energy.2018.03.180.

[5] D. O. Akinyele, R. K. Rayudu, Review of energy storage technologies for sustainable power networks, Sustainable Energy Technologies and Assessments 8 (2014) 74–91. doi:10.1016/j.seta.2014.07.004.
URL https://www.sciencedirect.com/science/article/pii/S2213138814000708

[6] Institute for Sustainable Process Technology, ISPT, Power to Ammonia, Tech. rep., ISPT (2017).
URL http://www.ispt.eu/media/ISPT-P2A-Final-Report.pdfhttp://www.ispt.eu/media/ISPT-P2A-Final-Report.pdf.

[7] B. Decourt, Weaknesses and drivers for power-to-X diffusion in Europe. Insights from technological innovation system analysis, International Jour-

nal of Hydrogen Energy 44 (33) (2019) 17411–17430. doi:10.1016/j.ijhydene.2019.05.149.

[8] C. Hank, A. Sternberg, N. Köppel, M. Holst, T. Smolinka, A. Schaadt, C. Hebling, H.-M. Henning, Energy efficiency and economic assessment of imported energy carriers based on renewable electricity, Sustainable Energy & Fuels 4 (5) (2020) 2256–2273. doi:10.1039/d0se00067a.

[9] A. Valera-Medina, H. Xiao, M. Owen-Jones, W. I. David, P. J. Bowen, Ammonia for power, Progress in Energy and Combustion Science 69 (2018) 63–102. doi:10.1016/J.PECS.2018.07.001.
URL https://www.sciencedirect.com/science/article/pii/S0360128517302320

[10] J. Armijo, C. Philibert, Flexible production of green hydrogen and ammonia from variable solar and wind energy: Case study of Chile and Argentina, International Journal of Hydrogen Energy 45 (3) (2020) 1541–1558. doi:10.1016/j.ijhydene.2019.11.028.

[11] K. E. Lamb, M. D. Dolan, D. F. Kennedy, Ammonia for hydrogen storage; A review of catalytic ammonia decomposition and hydrogen separation and purification, International Journal of Hydrogen Energy 44 (7) (2019) 3580–3593. doi:10.1016/J.IJHYDENE.2018.12.024.
URL https://www.sciencedirect.com/science/article/pii/S0360319918339272

[12] IEA (2019), The Future of Hydrogen, Paris,, 2019. doi:10.1787/1e0514c4-en.
URL www.iea.org/publications/reports/thefutureofhydrogen/.

[13] I. I. Cheema, U. Krewer, Operating envelope of Haber–Bosch process design for power-to-ammonia, RSC Advances 8 (61) (2018) 34926–34936. doi:10.1039/C8RA06821F.
URL http://xlink.rsc.org/?DOI=C8RA06821F

[14] C. Smith, A. K. Hill, L. Torrente-Murciano, Current and future role of Haber–Bosch ammonia in a carbon-free energy landscape, Energy & Environmental Science 13 (2) (2020) 331–344. doi:10.1039/c9ee02873k.

[15] M. Rovaglio, D. Manca, F. Cortese, P. Mussone, Multistability and robust control of the ammonia synthesis loop, Computer Aided Chemical Engineering 9 (C) (2001) 723–730. doi:10.1016/S1570-7946(01)80115-2.
URL https://www.sciencedirect.com/science/article/pii/S1570794601801152

[16] J. C. Morud, S. Skogestad, Analysis of instability in an industrial ammonia reactor, AIChE Journal 44 (4) (1998) 888–895. doi:10.1002/aic.690440414.
URL http://doi.wiley.com/10.1002/aic.690440414

[17] I. I. Cheema, U. Krewer, Optimisation of the Autothermal NH3 Production Process for Power-to-Ammonia, Processes 8 (1) (2019) 38. doi:10.3390/pr8010038.
URL https://www.mdpi.com/2227-9717/8/1/38

[18] R. Bañares-Alcántara, G. Dericks III, M. Fiaschetti, P. Grünewald, J. Masa Lopez, E. Tsang, A. Yang, L. Ye, S. Zhao, Analysis of Islanded Ammonia-based Energy Storage Systems, Tech. rep., University of Oxford, Oxford (2015).

[19] R. Nayak-Luke, R. Bañares-Alcántara, I. Wilkinson, "Green" Ammonia: Impact of Renewable Energy Intermittency on Plant Sizing and Levelized Cost of Ammonia, Industrial & Engineering Chemistry Research 57 (43) (2018) 14607–14616. doi:10.1021/acs.iecr.8b02447.
URL http://pubs.acs.org/doi/10.1021/acs.iecr.8b02447

[20] E. R. Morgan, J. F. Manwell, J. G. McGowan, Sustainable Ammonia Production from U.S. Offshore Wind Farms: A Techno-Economic Review, ACS Sustainable Chemistry & Engineering 5 (11) (2017) 9554–9567.

doi:10.1021/acssuschemeng.7b02070.
URL http://pubs.acs.org/doi/10.1021/acssuschemeng.7b02070

[21] E. Morgan, J. Manwell, J. McGowan, Wind-powered ammonia fuel production for remote islands: A case study, Renewable Energy 72 (2014) 51–61. doi:10.1016/j.renene.2014.06.034.

[22] A. Tripodi, M. Compagnoni, E. Bahadori, I. Rossetti, Process simulation of ammonia synthesis over optimized Ru/C catalyst and multibed Fe + Ru configurations, Journal of Industrial and Engineering Chemistry 66 (2018) 176–186. doi:10.1016/J.JIEC.2018.05.027.
URL https://www.sciencedirect.com/science/article/pii/S1226086X18302569

[23] A. Stephens, R. Richards, Steady state and dynamic analysis of an ammonia synthesis plant, Automatica 9 (1) (1973) 65–78. doi:10.1016/0005-1098(73)90013-7.
URL https://www.sciencedirect.com/science/article/pii/0005109873900137

[24] R. Maria Brigitte Gullberg, V. Alstad, Y. International ASA, Controllability Analysis of Ammonia Synthesis Loops, Tech. rep. (2018).
URL https://ntnuopen.ntnu.no/ntnu-xmlui/handle/11250/2580067

[25] T. Hasenkamp, T. Adler, A. Carlsson, M. Arvidsson, Robust design methodology in a generic product design process, Total Quality Management and Business Excellence (2007). doi:10.1080/14783360701231294.

[26] M. Reese, C. Marquart, M. Malmali, K. Wagner, E. Buchanan, A. McCormick, E. L. Cussler, Performance of a Small-Scale Haber Process, Industrial & Engineering Chemistry Research 55 (13) (2016) 3742–3750. doi:10.1021/acs.iecr.5b04909.
URL http://pubs.acs.org/doi/10.1021/acs.iecr.5b04909

[27] Z. K. Nagy, R. D. Braatz, Distributional uncertainty analysis using power series and polynomial chaos expansions, Journal of Process Control 17 (3) (2007) 229–240. doi:10.1016/j.jprocont.2006.10.008.

[28] D. Kumar, H. Budman, Robust nonlinear MPC based on Volterra series and polynomial chaos expansions, Journal of Process Control 24 (1) (2014) 304–317. doi:10.1016/j.jprocont.2013.03.003.

[29] D. Kumar, H. Budman, Applications of Polynomial Chaos Expansions in optimization and control of bioreactors based on dynamic metabolic flux balance models, Chemical Engineering Science 167 (2017) 18–28. doi:10.1016/j.ces.2017.03.035.

[30] G. Kimaev, L. A. Ricardez-Sandoval, A comparison of efficient uncertainty quantification techniques for stochastic multiscale systems, AIChE Journal 63 (8) (2017) 3361–3373. doi:10.1002/aic.15702.

[31] Y. Du, T. A. Duever, H. Budman, Generalized Polynomial Chaos-Based Fault Detection and Classification for Nonlinear Dynamic Processes, Industrial and Engineering Chemistry Research 55 (7) (2016) 2069–2082. doi:10.1021/acs.iecr.5b04694.

[32] Y. Xu, L. Mili, A. Sandu, M. R. Von Spakovsky, J. Zhao, Propagating Uncertainty in Power System Dynamic Simulations Using Polynomial Chaos, IEEE Transactions on Power Systems 34 (1) (2019) 338–348. doi:10.1109/TPWRS.2018.2865548.

[33] I. M. Cerrillo-Briones, L. A. Ricardez-Sandoval, Robust optimization of a post-combustion CO2 capture absorber column under process uncertainty, Chemical Engineering Research and Design 144 (2019) 386–396. doi:10.1016/j.cherd.2019.02.020.

[34] M. Tejeda-Iglesias, J. Szuba, R. Koniuch, L. Ricardez-Sandoval, Optimization and Modeling of an Industrial-Scale Sulfuric Acid Plant under Un-

certainty, Industrial and Engineering Chemistry Research 57 (24) (2018) 8253–8266. doi:10.1021/acs.iecr.8b00785.

[35] D. Coppitters, W. De Paepe, F. Contino, Robust design optimization and stochastic performance analysis of a grid-connected photovoltaic system with battery storage and hydrogen storage, Energy 213 (2020) 118798. doi:10.1016/j.energy.2020.118798.

[36] S. Giorgetti, C. Diederik, W. De Paepe, L. Bricteux, F. Contino, G. Aversano, A. Parente, Surrogate-assisted modeling and Robust Optimization of a micro Gas Turbine plant with Carbon Capture, in: Turbomachinery Technical Conference and Exposition GT2019, Phoenix (Arizona), USA, 2019, p. 11.
URL https://difusion.ulb.ac.be/vufind/Record/ULB-DIPOT:oai:dipot.ulb.ac.be:2013/282183/Holdings

[37] D. Coppitters, W. De Paepe, F. Contino, Surrogate-assisted robust design optimization and global sensitivity analysis of a directly coupled photovoltaic-electrolyzer system under techno-economic uncertainty, Applied Energy 248 (2019) 310–320. doi:10.1016/j.apenergy.2019.04.101.

[38] D. Chaffart, L. A. Ricardez-Sandoval, Robust dynamic optimization in heterogeneous multiscale catalytic flow reactors using polynomial chaos expansion, Journal of Process Control 60 (2017) 128–140. doi:10.1016/j.jprocont.2017.07.002.

[39] S. Bhonsale, P. Nimmegeers, D. Telen, J. A. Paulson, A. Mesbah, J. Van Impe, On the implementation of generalized polynomial chaos in dynamic optimization under stochastic uncertainty: a user perspective, in: Computer Aided Chemical Engineering, Vol. 46, Elsevier B.V., 2019, pp. 541–546. doi:10.1016/B978-0-12-818634-3.50091-6.

[40] G. D. Patron, L. Ricardez-Sandoval, A robust nonlinear model predic-

tive controller for a post-combustion CO2 capture absorber unit, Fuel 265 (2020) 116932. doi:10.1016/j.fuel.2019.116932.

[41] G. Makrygiorgos, G. M. Maggioni, A. Mesbah, Surrogate modeling for fast uncertainty quantification: Application to 2D population balance models, Computers and Chemical Engineering 138 (2020) 106814. doi:10.1016/j.compchemeng.2020.106814.

[42] G. Kimaev, D. Chaffart, L. A. Ricardez-Sandoval, Multilevel Monte Carlo applied for uncertainty quantification in stochastic multiscale systems, AIChE Journal 66 (8) (2020). doi:10.1002/aic.16262.

[43] J. A. Paulson, M. Martin-Casas, A. Mesbah Id, Fast uncertainty quantification for dynamic flux balance analysis using non-smooth polynomial chaos expansions (2019). doi:10.1371/journal.pcbi.1007308.

[44] P. Laššák, J. Labovský, . Jelemenský, Influence of parameter uncertainty on modeling of industrial ammonia reactor for safety and operability analysis, Journal of Loss Prevention in the Process Industries 23 (2) (2010) 280–288. doi:10.1016/J.JLP.2009.10.001.
URL https://www.sciencedirect.com/science/article/pii/S0950423009001673

[45] K. Verleysen, D. Coppitters, A. Parente, W. De Paepe, F. Contino, A. Parente, F. Contino, How can power-to-ammonia be robust? Optimization of an ammonia synthesis plant powered by a wind turbine considering operational uncertainties., Fuel 266 (2019) 117049. doi:10.1016/j.fuel.2020.117049.
URL https://linkinghub.elsevier.com/retrieve/pii/S0016236120300442

[46] A. Araújo, S. Skogestad, Control structure design for the ammonia synthesis process, Computers & Chemical Engineering 32 (12) (2008) 2920–2932. doi:10.1016/J.COMPCHEMENG.2008.03.001.

URL https://www.sciencedirect.com/science/article/pii/S0098135408000392

[47] D. Frattini, G. Cinti, G. Bidini, U. Desideri, R. Cioffi, E. Jannelli, A system approach in energy evaluation of different renewable energies sources integration in ammonia production plants, Renewable Energy 99 (2016) 472–482. doi:10.1016/j.renene.2016.07.040.
URL https://linkinghub.elsevier.com/retrieve/pii/S096014811630636X

[48] Ostuni, Method for load regulation of an ammonia plant (2008). arXiv:arXiv:1208.5721, doi:US2010/0311130Al.
URL https://patents.google.com/patent/US9463983B2/en

[49] G. F. Froment, J. De Wilde, K. B. Bischoff, Chemical reactor analysis and design, 3rd Edition, 2011.

[50] A. Tripodi, M. Compagnoni, R. Martinazzo, G. Ramis, I. Rossetti, Process Simulation for the Design and Scale Up of Heterogeneous Catalytic Process: Kinetic Modelling Issues, Catalysts 7 (5) (2017) 159. doi:10.3390/catal7050159.
URL http://www.mdpi.com/2073-4344/7/5/159

[51] A. Documentation Team, Aspen HYSYS Dynamic Modeling Guide, Tech. rep. (2006).
URL http://www.aspentech.com

[52] L. Ye, R. Nayak-Luke, R. Bañares-Alcántara, E. Tsang, Reaction: "Green" Ammonia Production, Chem 3 (5) (2017) 712–714. doi:10.1016/j.chempr.2017.10.016.
URL https://linkinghub.elsevier.com/retrieve/pii/S2451929417304448

[53] K. H. Rouwenhorst, A. G. Van der Ham, G. Mul, S. R. Kersten, Islanded

ammonia power systems: Technology review & conceptual process design (oct 2019). doi:10.1016/j.rser.2019.109339.

[54] N. Pernicone, F. Ferrero, I. Rossetti, L. Forni, P. Canton, P. Riello, G. Fagherazzi, M. Signoretto, F. Pinna, Wustite as a new precursor of industrial ammonia synthesis catalysts, Applied Catalysis A: General 251 (1) (2003) 121–129. doi:10.1016/S0926-860X(03)00313-2.
URL https://www.sciencedirect.com/science/article/pii/S0926860X03003132

[55] H. Bonnowitz, J. Straus, D. Krishnamoorthy, E. Jahanshahi, S. Skogestad, Control of the Steady-State Gradient of an Ammonia Reactor using Transient Measurements, in: Computer Aided Chemical Engineering, Vol. 43, Elsevier B.V., 2018, pp. 1111–1116. doi:10.1016/B978-0-444-64235-6.50194-7.

[56] G. Scheller, S. Krummeck, Measurement Uncertainty of a Temperature Measuring Chain, Tech. rep., JUMO Campus (2018).
URL https://bit.ly/2HYUcoL

[57] G. Gramatica, N. Pernicone, Kinetics of Ammonia Synthesis and Influence on Converter Design, 1991, pp. 211–252. doi:10.1007/978-1-4757-9592-9_6.
URL http://link.springer.com/10.1007/978-1-4757-9592-9{_}6

[58] I. Lee, K. K. Choi, L. Du, D. Gorsich, Dimension reduction method for reliability-based robust design optimization, Computers and Structures 86 (13-14) (2008) 1550–1562. doi:10.1016/j.compstruc.2007.05.020.

[59] T. Wu, Risk and reliability in geotechnical engineering, Georisk: Assessment and Management of Risk for Engineered Systems and Geohazards 9 (3) (2015) 218–219. doi:10.1080/17499518.2015.1070784.

[60] G. Blatman, B. Sudret, Efficient computation of global sensitivity indices

using sparse polynomial chaos expansions, Reliability Engineering and System Safety 95 (11) (2010) 1216–1229. doi:10.1016/j.ress.2010.06.015.

[61] Y. Qiu, J. Lin, X. Chen, F. Liu, Y. Song, Nonintrusive Uncertainty Quantification of Dynamic Power Systems Subject to Stochastic Excitations (jan 2020). arXiv:2001.06848, doi:10.1109/tpwrs.2020.3007746.
URL http://arxiv.org/abs/2001.06848

[62] E. Torre, S. Marelli, P. Embrechts, B. Sudret, Data-driven polynomial chaos expansion for machine learning regression, Journal of Computational Physics 388 (2018) 601–623. arXiv:1808.03216, doi:10.1016/j.jcp.2019.03.039.
URL http://arxiv.org/abs/1808.03216http://dx.doi.org/10.1016/j.jcp.2019.03.039

[63] S. Marelli, C. Lamas, B. Sudret, Uqlab user manual–sensitivity analysis.

[64] I. Dimov, R. Georgieva, Monte Carlo algorithms for evaluating Sobol' sensitivity indices, in: Mathematics and Computers in Simulation, Vol. 81, 2010, pp. 506–514. doi:10.1016/j.matcom.2009.09.005.

[65] G. Blatman, B. Sudret, Sparse polynomial chaos expansions and adaptive stochastic finite elements using a regression approach, Comptes Rendus - Mecanique 336 (6) (2008) 518–523. doi:10.1016/j.crme.2008.02.013.

[66] B. Sudret, Polynomial chaos expansions and stochastic finite element methods. Kok-Kwang Phoon, CRC Press, 2015.
URL https://hal.archives-ouvertes.fr/hal-01449883

[67] S. Abraham, M. Raisee, G. Ghorbaniasl, F. Contino, C. Lacor, A robust and efficient stepwise regression method for building sparse polynomial chaos expansions, Journal of Computational Physics 332 (2017) 461–474. doi:10.1016/J.JCP.2016.12.015.
URL https://www.sciencedirect.com/science/article/pii/S0021999116306684

[68] E. Haro Sandoval, F. Anstett-Collin, M. Basset, Sensitivity study of dynamic systems using polynomial chaos, Reliability Engineering and System Safety 104 (2012) 15–26. doi:10.1016/j.ress.2012.04.001.

[69] C. V. Mai, B. Sudret, Surrogate models for oscillatory systems using sparse polynomial chaos expansions and stochastic time warping, SIAM-ASA Journal on Uncertainty Quantification 5 (1) (2017) 540–571. arXiv:1609.09286, doi:10.1137/16M1083621.

[70] C. V. Mai, M. D. Spiridonakos, E. N. Chatzi, B. Sudret, Surrogate modelling for stochastic dynamical systems by combining NARX models and polynomial chaos expansions (apr 2016). arXiv:1604.07627.
URL http://arxiv.org/abs/1604.07627

[71] O. Maître, L. Mathelin, O. Knio, M. Hussaini, Asynchronous time integration for polynomial chaos expansion of uncertain periodic dynamics, Discrete and Continuous Dynamical Systems 28 (1) (2010) 199–226. doi:10.3934/dcds.2010.28.199.
URL http://www.aimsciences.org/journals/displayArticles.jsp?paperID=5069

[72] J. Eggins, L. Vu, Integration of MATLAB and LabVIEW with Aspen Plus Dynamics Using Control Strategies for a High-Fidelity Distillation Column, Tech. rep. (2015).

[73] K. Rabchuk, B. Lie, A. Mjaavatten, V. Siepmann, STABILITY MAP FOR AMMONIA SYNTHESIS REACTORS, Tech. rep. (2014).
URL http://www.greener-industry.org.uk/index.htm

[74] D. Flórez-Orrego, S. de Oliveira Junior, Modeling and optimization of an industrial ammonia synthesis unit: An exergy approach, Energy 137 (2017) 234–250. doi:10.1016/j.energy.2017.06.157.
URL https://linkinghub.elsevier.com/retrieve/pii/S0360544217311234

[75] G. Chehade, I. Dincer, Advanced kinetic modelling and simulation of a new small modular ammonia production unit, Chemical Engineering Science 236 (2021) 116512. doi:10.1016/j.ces.2021.116512.

[76] M. H. Khademi, R. S. Sabbaghi, Comparison between three types of ammonia synthesis reactor configurations in terms of cooling methods, Chemical Engineering Research and Design 128 (2017) 306–317. doi:10.1016/J.CHERD.2017.10.021.
URL https://www.sciencedirect.com/science/article/pii/S0263876217305865?via{%}3Dihub{#}fig0055

[77] A. Attari Moghaddam, U. Krewer, Poisoning of Ammonia Synthesis Catalyst Considering Off-Design Feed Compositions, Catalysts 10 (11) (2020) 1225. doi:10.3390/catal10111225.
URL https://www.mdpi.com/2073-4344/10/11/1225

[78] M. Valipour, K. M. Toffolo, L. A. Ricardez-Sandoval, State estimation and sensor location for Entrained-Flow Gasification Systems using Kalman Filter, Control Engineering Practice 108 (2021) 104702. doi:10.1016/j.conengprac.2020.104702.

[79] M. Valipour, L. A. Ricardez-Sandoval, Assessing the Impact of EKF as the Arrival Cost in the Moving Horizon Estimation under Nonlinear Model Predictive Control, Industrial and Engineering Chemistry Research 60 (7) (2021) 2994–3012. doi:10.1021/acs.iecr.0c06095.